

PAPER • OPEN ACCESS

Poisson's Ratio Distribution in A Geothermal Field

To cite this article: Muhammad Fawzy Ismullah Massinai *et al* 2019 *IOP Conf. Ser.: Earth Environ. Sci.* **279** 012025

View the [article online](#) for updates and enhancements.

Poisson's Ratio Distribution in A Geothermal Field

Muhammad Fawzy Ismullah Massinai¹, Basdar Purwansah BS², Muhammad Yustin Kamah³, Muhammad Altin Massinai^{1*}

¹Geophysics Dept., Hasanuddin University

²Professional Geoscience at PT. Pamapersada Nusantara

³Advisor at PT. Pertamina Geothermal Energy

*altin@science.unhas.ac.id

Abstract. Nowadays microearthquake or microseismic monitoring is powerful tool to investigate and evaluate the geothermal field. Each event of microseismic can be associated with permeable zone. One parameter can be used as a fracture indicator is Poisson's Ratio. The simple method to get information about Poisson's Ratio is Wadati Diagram. We applied this method in "A" Geothermal Field with 2 month recording microseismic data. The range of Poisson's Ratio distribution is 0.11197 – 0.468463. The lower Poisson's Ratio associated with un-fractured rocks and the higher indicate fractured rocks.

1. Introduction

Nowadays microearthquake or microseismic monitoring is powerful tool to investigate and evaluate the geothermal field. Many research used microseismic for that goal, such as: at Coso geothermal area, California [1]; at Lahendong Geothermal Field, North Sulawesi [2]; at Rotokawa Geothermal Field, New Zealand [3, 4, 5], at Okuaizu Geothermal Field, Japan [6]. Microseismic monitoring can give information about fracture characterization on geothermal field. Each event of microseismic can be associated with permeable zone. Understand fracture network characterization on geothermal field can give improvement on geothermal system. Good fracture networks signed by fracture connectivity until fluids migrate from injection well to reservoir or from reservoir to production well. Common microseismic mechanisms cited in literature are fluid pressure or temperature perturbations, reservoir volume changes, or chemical changes associated with extraction and/ or injection [5]; illustrated by Fig.1.

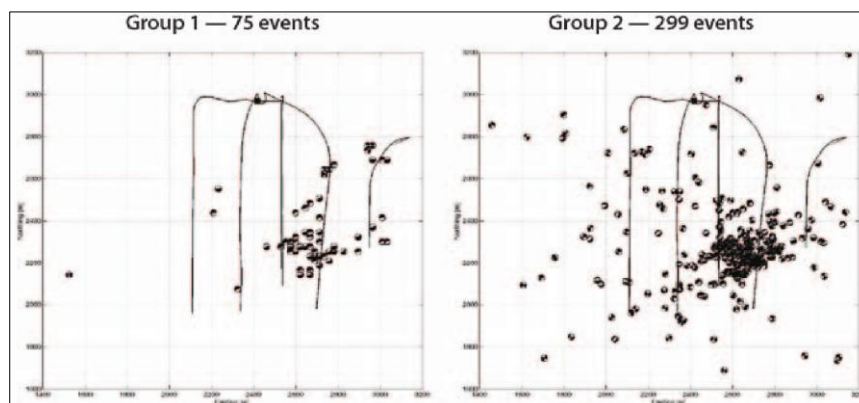


Figure 1. Group 2 is microseismic group after injection in Group 1. Dot is microseismic and line is wells [7].

As a result, this geophysical method is very helpful to develop a geothermal field. Poisson's ratio is one of the important parameters that can be used as a fracture indicator through simple calculation of Wadati Diagram. Whereas, well data like cores, minerals and loss circulation can provide reservoir permeability are very expensive and limited [2].

Wadati Diagram indicate different fracture intensity between shallow and deep reservoir. This paper explains Poisson's ratio derived from 2 month recording microseismic data at the "A" geothermal field.

2. The "A" Geothermal Field

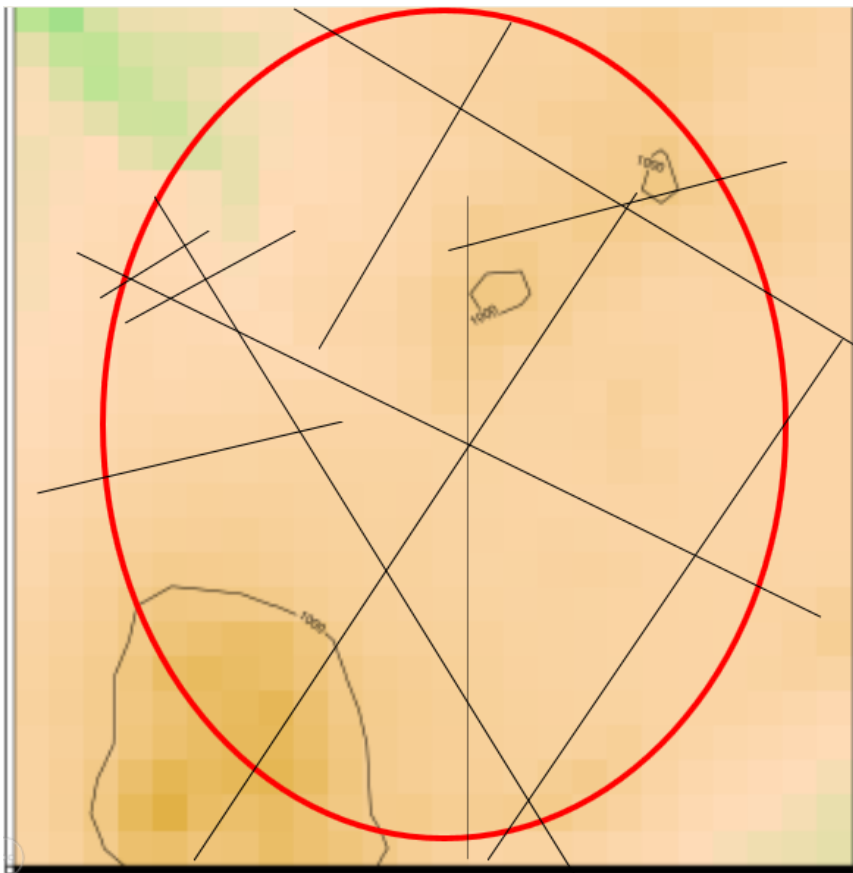


Figure 2. Map of "A" geothermal field. Red circle is location and black line are fault. Coordinate is hidden.

The "A" geothermal field is land at ± 750 msl and as part of volcano-tectonic depression. Volcanoes around this geothermal with southwest to northeast. Geology main feature is caldera with 4 km diameter. This caldera limited by normal fault on its southwest [8]

Fault on research area dominated by normal fault such as R Fault, Li Fault, TP Fault, SK Fault, PU Fault, TU Fault and Le Fault (Fig. 2). Geothermal manifestation located around R Fault. This fault is normal fault and many feature indicated high alteration in this location. Other geothermal manifestation located around TP Fault. All fault may affected by regional tectonic which formed depression on this area [8].

Main factor of geothermal reservoir is permeability. Reservoir system of this geothermal field divided into two system; northern and southern. In southern have $300 - 350^{\circ}\text{C}$ temperature with 80% dry steam. In others, have lower around $250 - 280^{\circ}\text{C}$ temperature with 30% dry steam. They separated by N - S structure and assumed as pressure barrier. Well data indicated shallow reservoir. This reservoir

found around 400 – 700 m depth. At W-1 and W-2, (Fig. 3) reservoir found around 650 m depth and W-4 and W-5 showed lateral current from shallow aquifer [8].

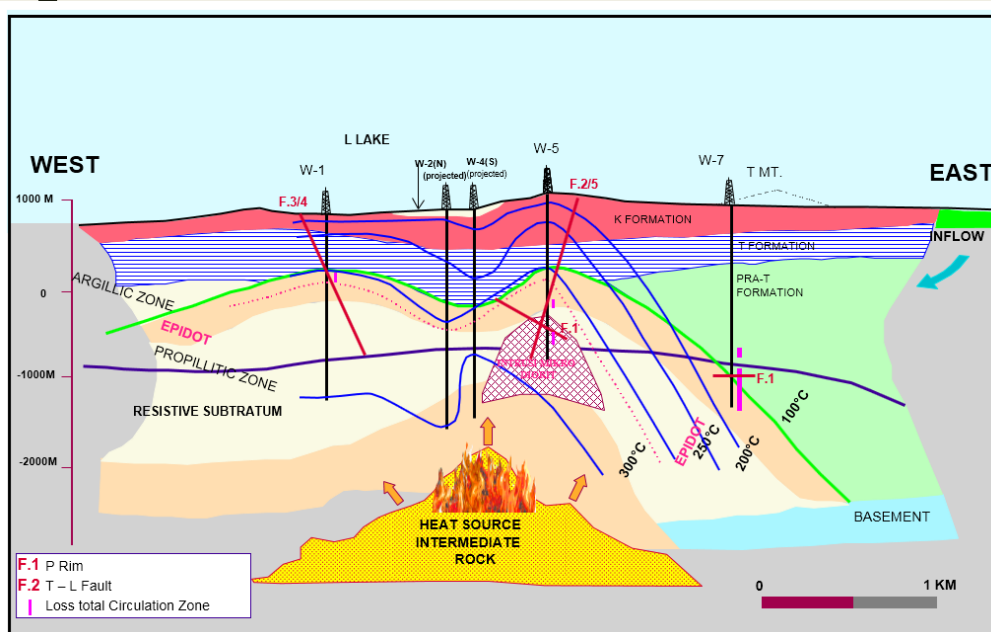


Figure 3. The A geothermal field model, modified from [8].

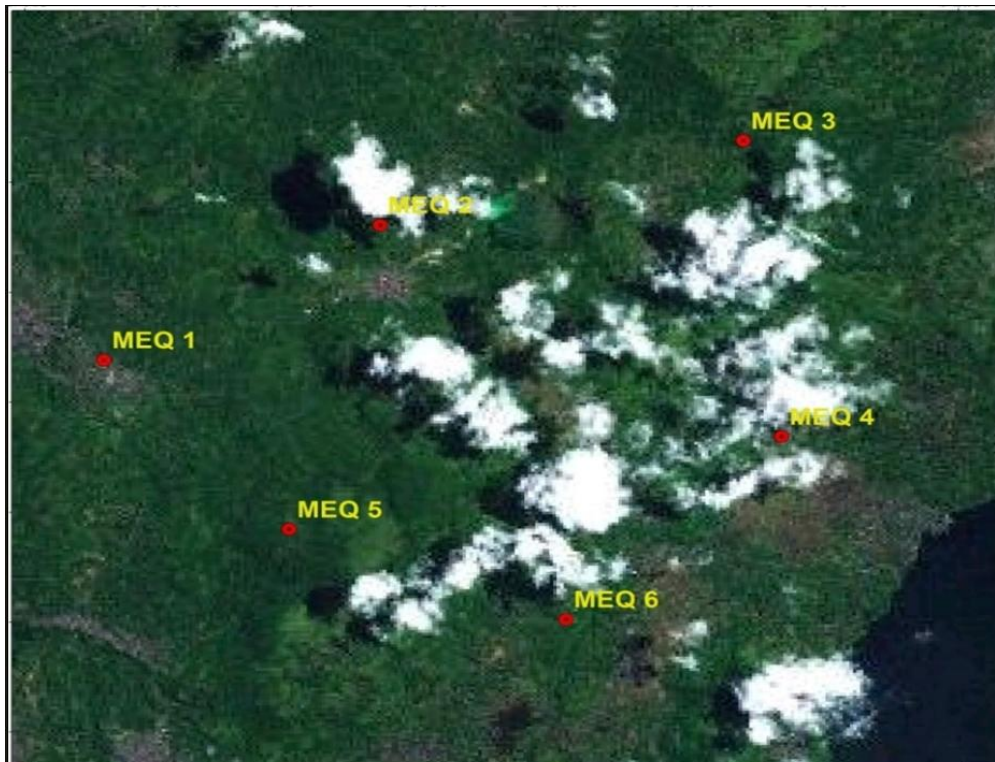


Figure 4. Distribution of seismograph [8]. Coordinate is hidden.

Generally in geothermal Field, the typical microseismic, follow: duration under 50 second, the depths under 5 km, and the P and S arrival (S-P) time differences under 3 second. Therefore, a simple assumption that model is a horizontal layered velocity structure, assuming constant, isotropic velocity within one layer, is reasonable enough to get a quick interpretation as preliminary result [2].

A small error in picking of the arrival time and the inaccuracies of velocity model can produce a large error in determining the hypocenter and epicenter location. Therefore, both factors must be controlled, carefully [2].

Microseismic activity observed continue and real time by Pertamina Geothermal Energy (PGE) used 6 digital seismograph (Fig. 4) with GPS to synchronize time and position. The data on this research area microseismic data on September – October 2010 periods. This research used 14 event microseismic [8].

3. Wadati Diagram

Wadati diagram is important in processing micro-earthquake data for two reasons. The first is that we can control the correct picks of travel time of P wave and S wave (t_s and t_p) from record data. The second reason is that we can compare the origin time of earthquake (T_o , if the time of S and P are equal, it means the rock are fractured) with t_o from a computer program e.g. linier inversion [2].

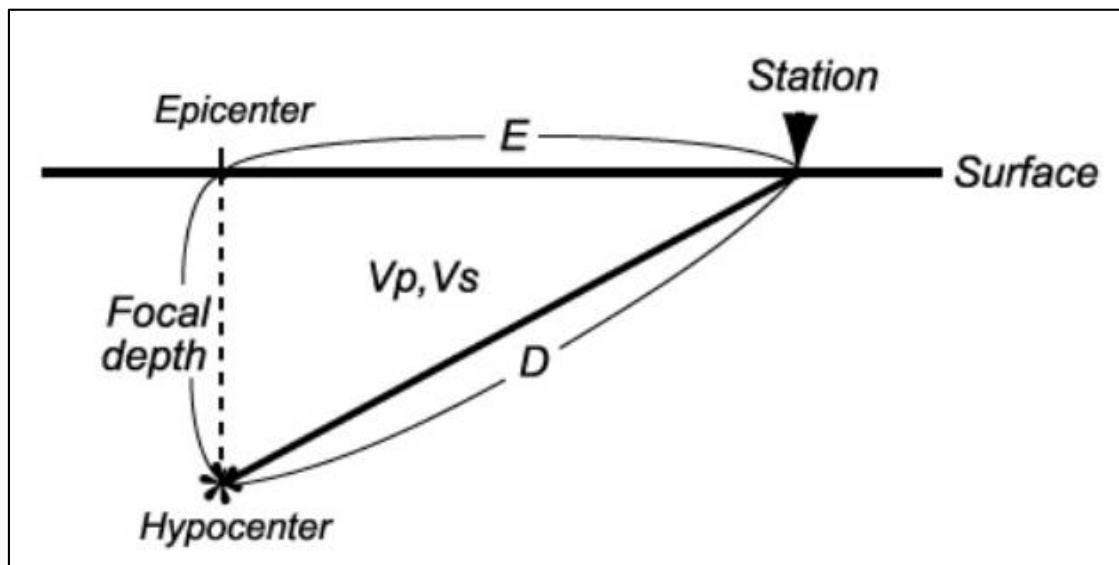


Figure 5. Illustration of hypocenter to get Wadati Diagram concept. E is epicenter distance and D is hypocenter distance [9].

The principle of the Wadati diagram is as follows, assuming that the medium is homogeneous. A hypocentral distance is represented by P- and S-wave travel times and velocities as follows:

$$D = (T_p - T_o) * V_p = T_p * V_p \quad (1)$$

$$D = (T_s - T_o) * V_s = \{(T_s - T_p) + (T_p - T_o)\} * V_s = \{(T_s - T_p) + T_p\} * V_s \quad (2)$$

From equations (1) and (2)

$$T_p * V_p = \{(T_s - T_p) + T_p\} * V_s \quad (3)$$

$$T_p * (V_p - V_s) = (T_s - T_p) * V_s \quad (4)$$

Therefore

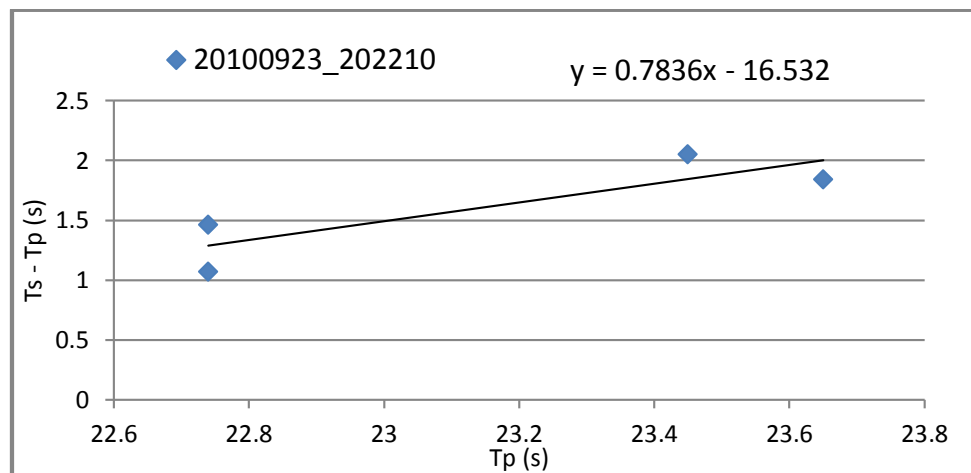
$$(T_s - T_p) = \left(\frac{V_p}{V_s} - 1\right) * T_p \quad (5)$$

This is also valid in a layered media with a constant V_p/V_s ratio [9].

The T_p and T_s picked data from one microseismic event as shown in Tabel-1 as example to all microseismic event. The next step is constructing a Wadati diagram by plotting all $T_s - T_p$ vs T_p for all stations, as shown in Fig. 6.

Table 1. Tp and Ts picked data from one microseismic event

No	Station		Tp (s)	Ts (s)	Ts – Tp (s)
1	MEQ2	22	23.45	25.5	2.1
2	MEQ3	22	22.74	24.2	1.5
3	MEQ4	22	22.74	23.8	1.1
4	MEQ5	22	23.65	25.5	1.8

**Figure 6.** Wadati Diagram from data on Table 1.

Look linear regression equation of Fig. 6. V_p/V_s is the gradient + 1. So, from this Wadati Diagram got the V_p/V_s , is 1.7836.

4. Poisson's Ratio

Basically Poisson's ratio is defined by the ratio of the strain perpendicular to either type of deforming force to that in the direction of the force itself. In other way, by using compressional velocity and transversal velocity or the comparison of both velocity from Wadati diagram the Poisson's ratio is defined as follow [2]:

$$\sigma = \frac{(V_p^2 - 2V_s^2)}{2(V_p^2 - V_s^2)} \quad (6)$$

here σ , V_p dan V_s are Poisson's ratio, the compressional wave velocity (longitudinal) and the shear wave velocity (transversal) respectively [2].

If we assume that the ray-paths are confined to homogeneous geology, experimental and theoretical results indicate that additional fracturing of a fluid-filled rock will cause an increase in the Poisson's ratio. The P-wave velocity decreases slightly and the S-wave velocity significantly reduced [2].

The study from [2] got that in the steam dominated system, V_p decreases faster than V_s . The two parameters provide poisson ratio lower than 0.25. In the water dominated system at the higher porosity pressure, the Poisson's ratio is bigger than 0.25. The V_s decreases faster than V_p [2].

The Poisson's ratio of the A geothermal field is 0.11197 – 0.468463. The results indicate a differences between shallower and deeper zone. In the shallower zone, the Poisson's ratio dominated 0.2 up to 0.46, the anomalies gave on 0.125 – 0.144. In the deeper zone, the Poisson's ratio varies from 0.137 to 0.291, please look Fig. 7.

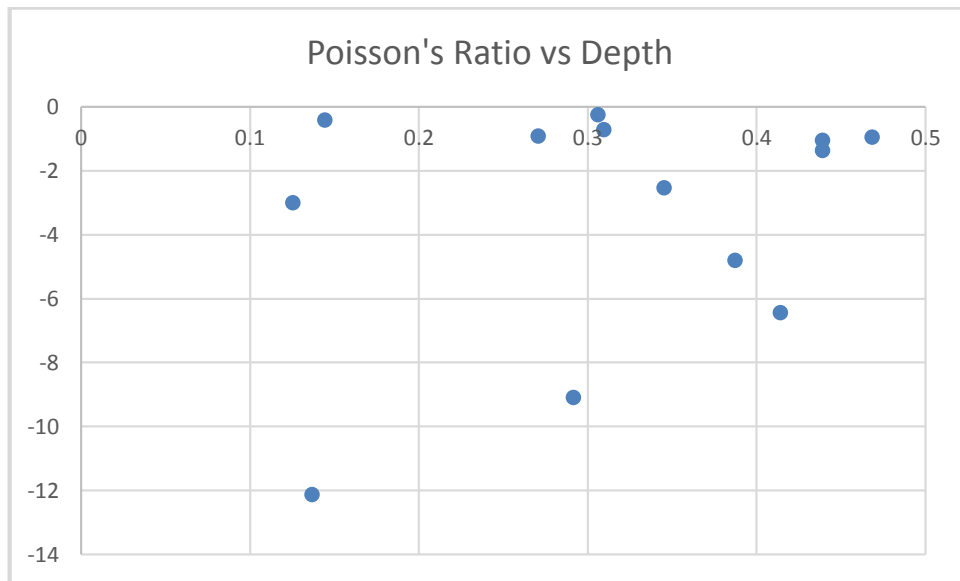


Figure 7. Poisson's ration of the A geothermal filed versus depth.

Figure 8 shows the significant differences between Poisson's ratio in the shallower zone and deeper zone. The value of Poisson's ratio with depth in the A geothermal field can be divided into two zones which correspond to shallower and deeper zone. The shallower zone with interval of Poisson's ratio varies from 0.2 up to 0.46 has depth from surface to 6500 meter depth and the deeper zone with interval of Poisson's ratio varies from 0.137 to 0.291 has depth is deeper than 6500 meter. Based on Fig. 8, the shallower zone is distinguished by the intensively fractured rock, soft and poorly consolidated. For the deeper is hard, rigid and it can interpreted as un-fractured rock.

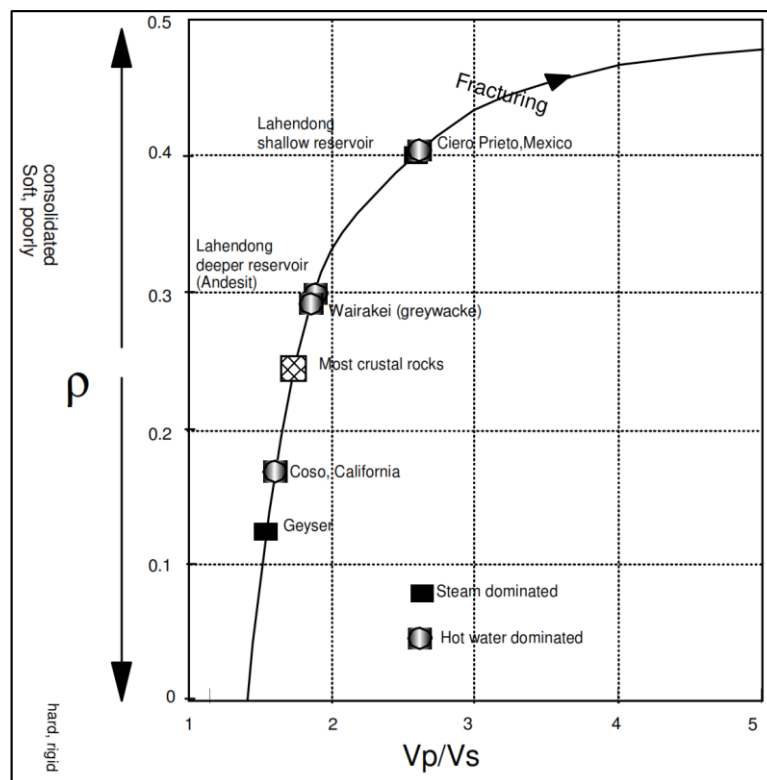


Figure 8. Poisson's ratio of some geothermal fields over the world wide versus Vp/Vs [2].

5. Conclusions

Based on the results, we had been conclude that:

1. Lower Poisson's ratio is associated with shallower zone, is distinguished by the intensively fractured rock, soft and poorly consolidated.
2. Higher Poisson's ratio is associated with deeper zone, is hard, rigid and it can interpreted as unfractured rock.

In the next step, the study will continue for determining hypocenter to get more accuracy in this result. The result in this study effectively to observe the relation between the Poisson ration and fracture intensity in geothermal field.

6. References

- [1] Lees J M & Wu H 2000 *Journal of Volcanology and Geothermal Research* **95** 157 – 173.
- [2] Silitonga T H, Siahaan E E, Suroso 2005 *Proc. World Geothermal Congress (Antalya)* p.1 – 10.
- [3] Bannister S, Sherburn S, Powell T, Bowyer D 2008 *Geothermal Resources Council – Transactions* **32** 259 – 263.
- [4] Sewell S M, Cumming W, Bardsley C J, Winick J, Quinao J, Wallis I C, Sherburn S, Bourguignon S, Bannister S 2015 *Proc. World Geothermal Congress (Melbourne)* p.1 – 10.
- [5] Sherburn S, Sewell S M, Bourguignon S, Cumming W, Bannister S, Bardsley C, Winick J, Quinao J, Wallis I C 2015 *Geothermics* **54** 23 – 34.
- [6] Okamoto K, Yi L, Asanuma H, Okabe T, Abe Y, Tsuzuki M 2018 *Earth Planets and Space* **70**:15.
- [7] Staněk F, Jechumtálová Z and Eisner L 2015 *Reservoir stress from microseismic source mechanisms* (The Leading Edge: August 2015)
- [8] Purwansah B 2012 *Bachelor Thesis* (unpublished, Geophysics Hasanuddin University).
- [9] Hurukawa N 2008 *Practical Analyses of Local Earthquakes*. International Institute of Seismology and Earthquake Engineering (IISEE) Building Research Institute, Tsukuba, Japan.

Acknowledgements

We gratefully acknowledge the USGS and BMKG for data. We thank to Geophysics Study Program, Faculty of Mathematics and Natural Science Hasanuddin University (UNHAS) for supporting this research.